AGU PUBLICATIONS

Geophysical Research Letters

RESEARCH LETTER
10.1002/2016GL069595

Key Points:
- First time daily satellite maps of SSS are obtained in the Mediterranean Sea
- Satellite SSS maps derived from SMOS capture the signal of fresh-core coastal eddies
- Use of satellite SSS maps allows to correctly retrieve the vorticity of Algerian eddies

Supporting Information:
- Supporting Information S1
- Movie S1
- Data Set S1

Correspondence to:
J. Isern-Fontanet,
jisern@icm.csic.es

Citation:
Isern-Fontanet, J., E. Olmedo, A. Turiel, J. Ballabrera-Poy, and E. García-Ladona (2016), Retrieval of eddy dynamics from SMOS sea surface salinity measurements in the Algerian Basin (Mediterranean Sea), *Geophys. Res. Lett.*, *43*, 6427–6434, doi:10.1002/2016GL069595.

Received 19 APR 2016
Accepted 24 MAY 2016
Accepted article online 28 MAY 2016
Published online 24 JUN 2016

Retrieval of eddy dynamics from SMOS sea surface salinity measurements in the Algerian Basin (Mediterranean Sea)

Jordi Isern-Fontanet[1], Estrella Olmedo[1], Antonio Turiel[1], Joaquim Ballabrera-Poy[1], and Emilio García-Ladona[1]

[1] Institut de Ciències del Mar (CSIC), Barcelona, Spain

Abstract The circulation in the Algerian Basin is characterized by the presence of fresh-core eddies that propagate along the coast or at distances between 100 and 200 km from the coast. Enhancements in the processing of the Soil Moisture and Ocean Salinity (SMOS) data have allowed to produce, for the first time, satellite sea surface salinity (SSS) maps in the Mediterranean Sea that capture the signature of Algerian eddies. SMOS data can be used to track them for long periods of time, especially during winter. SMOS SSS maps are well correlated with in situ measurements although the former has a smaller dynamical range. Despite this limitation, SMOS SSS maps capture the key dynamics of Algerian eddies allowing to retrieve velocities from SSS with the correct sign of vorticity.

1. Introduction

Horizontal surface density gradients in the ocean are responsible for surface geostrophic currents on scales where Earth rotation is important. These currents are systematically computed using along-track altimetric measurements of sea surface height (SSH), but the limited number of altimeters can lead to errors in their location [*Pascual et al.*, 2006]. On the other side, satellite measurements of sea surface temperature (SST) are better suited to locate flow patterns under the appropriate environmental conditions and can be exploited to retrieve density anomalies and, thus, velocities at the ocean surface through the Surface Quasi-Geostrophic (SQG) approach [*Isern-Fontanet et al.*, 2006a]. Nevertheless, in some areas salinity contribution to density may dominate over temperature contribution, which can induce wrong signs in the vorticity retrieved from SST. This situation can be found in the Algerian Basin [*Isern-Fontanet et al.*, 2014], which is located at the entrance of the Mediterranean Sea. The launch of the European Space Agency (ESA) Soil Moisture and Ocean Salinity (SMOS) satellite mission pioneered the measurements of sea surface salinity (SSS) from space [*Mecklenburg et al.*, 2015]. However, processing issues have impeded the generation of SSS maps in the Mediterranean Sea to capture key ocean features such as the Algerian eddies [*Font et al.*, 2013].

The Mediterranean Sea, a hot spot for climate change [*Giorgi*, 2006], is characterized by an excess of evaporation over precipitation and river runoff, which is compensated by the entrance of fresher waters from the Atlantic. These incoming waters spread through the basin, affecting its surface circulation [e.g., *Millot and Taupier-Letage*, 2005]. In the Algerian Basin, Atlantic waters form a well defined eastward coastal current that can become unstable, generating fresh-core coastal eddies that propagate downstream. These eddies can detach from the coast but remain trapped in the basin following relatively well defined patterns at distances ~100–200 km away from the coast [*Isern-Fontanet et al.*, 2006b]. The eddy activity in the region enhances the mixing of the recently entered fresher Atlantic waters with the saltier ambient ones, strongly affecting the spatial distribution of salinity and, therefore, playing a major role in the surface circulation of the Mediterranean Sea [see *Isern-Fontanet et al.*, 2004, and reference therein]. The dynamics of these Algerian eddies were mainly investigated using SSH and SST [e.g., *Taupier-Letage et al.*, 2003]. However, *Isern-Fontanet et al.* [2014] showed that the direct application of the SQG framework to retrieve currents from SST has some limitations in the Algerian basin due to the seasonal change of the relative orientation of SST and SSS gradients [e.g., *Puillat et al.*, 2002].

Recent studies have demonstrated the potential of new satellite measurements of SSS to describe features not well captured by SST maps such as fresh-core Gulf String rings [*Reul et al.*, 2014; *Umbert et al.*, 2015]. However, eddies in the Algerian Basin are more difficult to detect by SMOS because they are attached to the coast or located at distances from coast were the contamination from land in the L band microwave is important

[*Font et al.*, 2013]. In this study we show that new improvements in the processing of SMOS data (E. Olmedo et al., Enhanced retrieval of the geophysical signature of SMOS SSS maps, submitted to *Remote Sensing of Environment*, 2016) and the exploitation of the synergy between SSS and SST fields [*Umbert et al.*, 2014] lead to the detection of Algerian eddies in SSS maps and, consequently, to the improvement of ocean currents retrieval using SMOS measurements.

2. Data and Procedures

Three years (2011 – 2013) of SSS maps have been derived from L1B Brightness Temperature (Tb) products measured by SMOS and provided by ESA. First, Tb have been geolocalized in 25 km Lambert Azimuthal grid and corrected for the atmospheric, galactic, Sun glint, and roughness contributions [*Font et al.*, 2013]. After that, debiased, non-Bayesian L2 SSS anomalies have been derived using the methodology proposed by Olmedo et al. (submitted manuscript, 2016). Finally, absolute L2 SSS have been generated by adding the annual climatology from the World Ocean Atlas (WOA) [*Zweng et al.*, 2013]. Moreover, daily Reynolds SST [*Reynolds et al.*, 2007] provided by NOAA and Absolute Dynamic Topography (ADT) maps generated by AVISO [*AVISO Altimetry*, 2012] have been used. ADT maps have optimized parameters for the Mediterranean Sea and use the regional Mean Dynamic Topography computed by *Rio et al.* [2014]. For validation purposes, near surface in situ measurements provided by Argo floats from Coriolis have been used.

L2 SSS derived from SMOS measurements have been used to build SSS maps using a two-step procedure. In a first step, SMOS SSS daily L3 maps at 1/4° × 1/4° resolution have been produced by means of a successive corrections analysis applied over time periods of 9 days using the same influence radii as in WOA [*Zweng et al.*, 2013]. The time window in L3 maps has been chosen as 3 times SMOS revisit period (3 days), which provides good enough global coverage. These L3 maps are generated on a daily basis. The second step of the procedure aims at reducing the noise level and increasing the time resolution by applying multifractal fusion [*Umbert et al.*, 2014], combining 9 day L3 SSS maps with daily SST maps. Previous studies unveiled the strong correlation between SST and SSS gradients in the Algerian Basin, which suggests that both fields share information [e.g., *Millot and Taupier-Letage*, 2005]. Indeed, all ocean scalars sharing the same multifractal structure should verify that their gradients are related by means of a smooth matrix field, which led to the multifractal fusion technique proposed by *Umbert et al.* [2014]. In this study, we have used the modified version of this technique proposed by *Olmedo et al.* [2016] to merge L3 SSS maps with Reynolds SST maps at 1/4° ×1/4° and generate daily L4 SSS maps. The domain of influence taken into account to produce SSS maps has been restricted to the western Mediterranean.

3. Results

An assessment of the quality of the SSS maps in the Algerian Basin ((2°W,10°E) × (36°N,40°N)) is obtained by comparing them to in situ measurements provided by Argo floats. First of all, salinities from L4 SSS maps have been spatially interpolated onto Argo positions. Then, the values of Argo near-surface salinity have been discretized by bins with a bin width of 0.01 (see Figure 1). The central SMOS measure for each bin is the average of all values of SMOS SSS lying inside that bin, while the central Argo measure corresponds to the middle point of the bin. When analyzing such central measures, the averaged linear correlation between SMOS and Argo is 0.73. In addition, this linear correlation increases with the bin size, for example, the correlation becomes 0.87 for a bin size of 0.03. The sensitivity of SMOS SSS to salinity variations is being assessed by averaging the standard deviation of all bins, which is 0.15. The comparison between satellite and in situ measurements is also underlining that L4 SSS maps have a smaller dynamic range than Argo salinities (Figure 1). The scale factor between satellite and in situ salinities has been estimated in two different ways. For the first way, it has been taken as the quotient between the range of observed Argo salinities and the range of averaged SMOS salinities giving a scale factor of 3.20. For the second way, it has been taken as the slope of the linear regression between Argo salinities and the averaged SMOS salinities, which yields a smaller scale factor of 2.58. Finally, we have computed the standard deviation of the differences between salinities measured in situ and salinities interpolated from L4 SSS maps, which is 0.39 considering only those salinities that have a physical meaning in the Mediterranean Sea, i.e., $S \leq 40$.

A qualitative comparison between L4 SSS and SSH (ADT) maps is revealing a good coherence between structures at scales shorter than a few hundred kilometers (Figure 2). This is evident for the two fresh-core patterns approximately centered at 37.3°N,2°E and 37.5°N,7.5°E that correspond to anticyclonic vortices (SSH increases

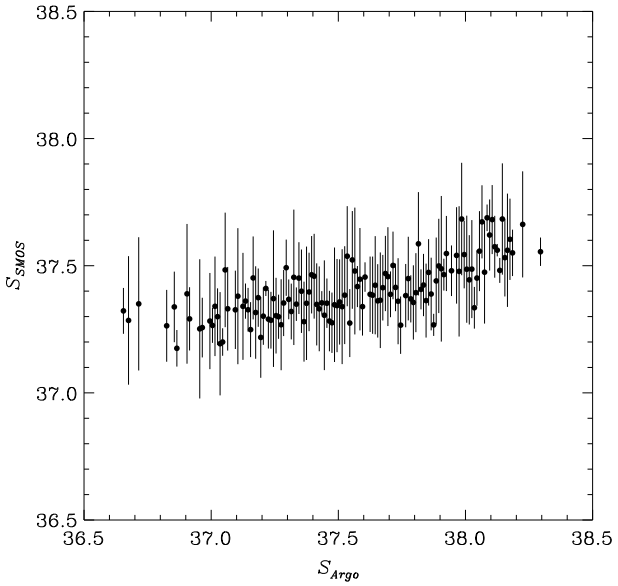

Figure 1. Scatterplot of binned SSS observations. Dots correspond to the mean value of salinity from SMOS SSS maps within each bin of in situ salinities from Argo and vertical lines corresponds to their standard deviation.

toward the eddy center). Furthermore, the westernmost eddy has been tracked from 3 January to 4 March featuring an eastward propagation along the coast and its splitting into two eddies (see the supporting information). The SSS signature of this eddy and its evolution have been found to be in agreement with SSH maps. In addition, it has been observed that some SSS signatures coincident with SSH structures are unnoticed in SST. Nevertheless, some caveats are being observed: the temporal variability of salinity in L4 SSS maps is sometimes too fast, some eddies that are observed in SSH and SST are not always captured by the SSS field, and some potential artifacts may still be present.

To further analyze the geophysical consistence of SST, SSS, and SSH, the three fields have been interpolated onto a common grid. Then, vorticity has been calculated from SSH (η) as

$$\zeta(\vec{x}) = \frac{g}{f_0}\nabla^2\eta(\vec{x}), \tag{1}$$

where $\nabla = (\partial_x, \partial_y)$, $g = 9.8$ ms^{-1} is gravity and $f_0 = 8.95\,10^{-5}$ s^{-1} the Coriolis parameter. Finally, SST, SSS, and vorticity anomalies (T', S', and η', respectively) have been computed by applying a band-pass filter with cutoff wavelengths equal to 100 km and 300 km. Vorticity is invariant under Galilean transformations, which facilitates the identification of patterns when strong larger-scale flows are present. Band-passed vorticity unveils the presence of some structures increasing the qualitative agreement between vorticity and SSS anomalies for the smallest structures (Figure 2). This is evident for the anticyclonic structure ($\zeta' < 0$) observed in SSH centered at 39.2°N, 6.2°E that was obscured by the presence of a nearby cyclonic structure ($\zeta' > 0$) seen in the vorticity field around 38.5°N, 7°E, which is in a good correspondence with SSS anomalies and, to a lesser extent, with SST anomalies. In general, in all the processed maps the patterns of SSS anomalies tend to be correlated with SST anomalies although the sign of this correlation can change as discussed in the introduction.

A quantitative comparison between L4 SSS and SSH maps involves an objective definition of a vortex to be able to extract their properties. Since Algerian eddies are anticyclonic fresh-core vortices, we are focusing on the identification of vortex cores with negative vorticity. Therefore, vortex cores have been identified in altimetric SSH maps using the procedure proposed by *Isern-Fontanet et al.* [2003] and *Isern-Fontanet et al.* [2006b]: a vortex core is a simply connected region with values of the Okubo-Weiss (W) parameter smaller than $-0.2\sigma_W$ and the same sign as vorticity, where σ_W is the spatial standard deviation of W. The Okubo-Weiss parameter has been computed from SSH as

$$W(\vec{x}) = 4\frac{g^2}{f_0^2}\left[\left(\frac{\partial^2\eta}{\partial x\partial y}\right)^2 - \left(\frac{\partial^2\eta}{\partial x^2}\right)\left(\frac{\partial^2\eta}{\partial y^2}\right)\right]. \tag{2}$$

This definition captures the core of Algerian eddies, which is characterized by very small isopycnal salinity gradients, while the surrounding cell of these eddies is characterized by a strong slope of isohalines with respect to isopycnals, an indication of intense mixing of fresh waters with the denser ambient waters [*Isern-Fontanet et al.*, 2004]. Once anticyclonic vortex cores have been identified in SSH fields, the probability density functions of negative anomalies S' and T' inside and outside anticyclonic vortex cores have been

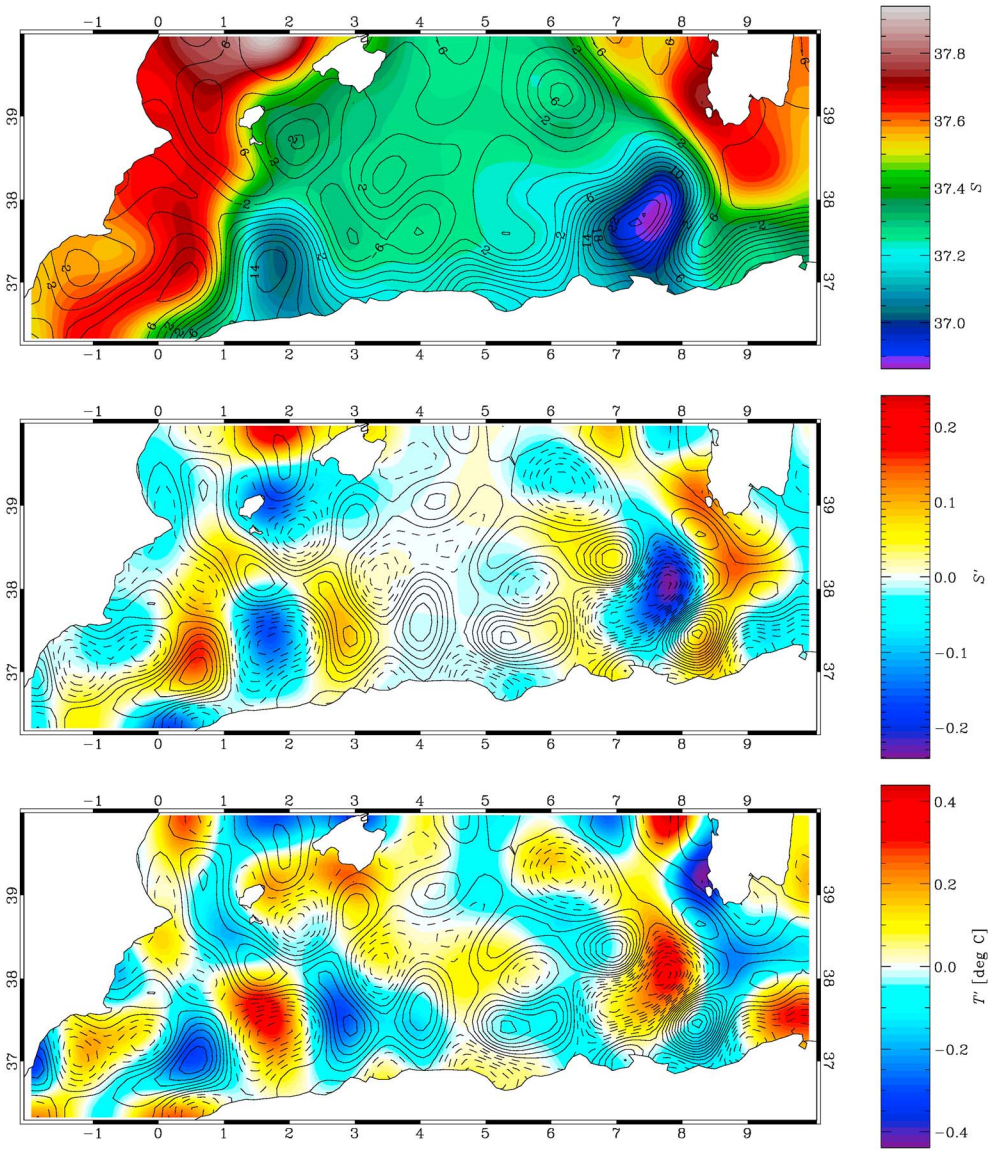

Figure 2. Snapshot of (top) SSS, (middle) SSS anomaly (S'), and (bottom) SST anomaly (T') corresponding to 6 January 2013. Solid lines in Figure 2 (top) correspond to SSH. In Figures 2 (middle) and 2 (bottom) maps black lines indicate positive (solid) and negative (dashed) vorticity isolines estimated from SSH.

evaluated monthly to unveil any seasonal variability. Results show that the probability of having negative SSS anomalies inside anticyclonic eddies in winter is significantly larger than 0.5 ($\sim$ 0.7, see Figure 3), while the probability of having negative anomalies outside eddies is $\sim$0.5. Some further insight is being obtained by analyzing the probability of having negative SST anomalies inside vortex cores. As shown in Figure 3, this probability is very low in winter ($\sim$ 0.25), indicating that the Okubo-Weiss criterion mainly captures warm-core vortices. The probability of having negative SSS (SST) anomalies inside the eddy core drops (grows) to $\sim$0.5 in summer, similar to the probability for the region outside anticyclonic vortex cores.

One key dynamical variable for the description of ocean flows is buoyancy $b(\vec{x})$, which can be approximated as

$$b(\vec{x}) \approx -g\rho_0^{-1}\left[\alpha\left(T(\vec{x}) - T_0\right) + \beta\left(S(\vec{x}) - S_0\right)\right], \tag{3}$$

where $\alpha < 0$ and $\beta > 0$ are the thermal expansion coefficient and the haline contraction coefficient, respectively, computed from the Equation of State for Seawater and T_0, S_0, and ρ_0 are a reference temperature,

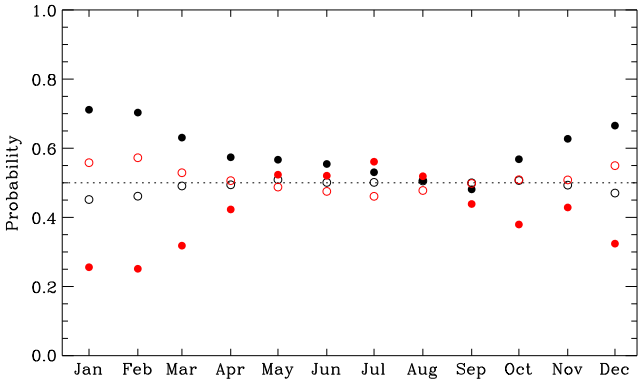

Figure 3. Seasonal evolution of the probability of finding negative salinity (black) and temperature (red) anomalies within an anticyclonic eddy core (solid dots) and outside eddy cores (circles).

salinity, and density. The evaluation of the contribution of temperature and salinity to buoyancy gradients is commonly done using the complex ratio given by

$$r(\vec{x}) = \frac{\alpha \nabla_i T}{\beta \nabla_i S} = |r(\vec{x})| e^{i\theta(\vec{x})}, \qquad (4)$$

where i is the imaginary unit and $\nabla_i \equiv \partial_x + i\partial_y$ [see *Isern-Fontanet et al.*, 2014, and references therein]. The phase $\theta(\vec{x})$ of the complex ratio $r(\vec{x})$ quantifies the degree of alignment of salinity and temperature gradients and the magnitude $|r(\vec{x})|$ their relative strength. The above ratio has been computed within anticyclonic cores observed during winter months (December–March). The results show that the probability of observing $|r| < 1$ is 0.7, implying that even without correcting the smaller dynamic range of SSS maps, buoyancy gradients within Algerian eddies are dominated by salinity. Moreover, during winter the contribution of SST and SSS to buoyancy gradients tend to reinforce each other; i.e., SST and SSS gradients have opposite signs, as suggested by the probability of having $|\theta| < \pi/4$ which is 0.58. On the contrary, during other periods of the year both contributions may tend to compensate as shown in the example of Figure 4.

Under the appropriate environmental conditions, the surface stream function $\psi(\vec{x})$ can be derived from surface buoyancy as [*Isern-Fontanet et al.*, 2014]

$$\hat{\psi}(\vec{k}) = F(k)\hat{b}(\vec{k}), \qquad (5)$$

where $\hat{(\,)}$ stands for the Fourier transform, $\vec{k}$ is the wave number vector, $k = |\vec{k}|$, and $F(k)$ is a transfer function that can be theoretically derived using the Quasi-Geostrophic Potential Vorticity equation, which becomes the classical SQG solution if constant stratification is assumed, i.e., $F(k) \sim k^{-1}$ [e.g., *LaCasce and Mahadevan*, 2006; *Lapeyre and Klein*, 2006]. If only SST is available, equation (5) can be modified to retrieve the stream function from SST [see *Isern-Fontanet et al.*, 2006b, 2008]. Alternatively, if SSH measurements are available, the transfer function can also be empirically determined imposing that the stream function spectra is that of SSH while the complex phase is that of SSS or SST [see *Isern-Fontanet et al.*, 2014; *González-Haro and Isern-Fontanet*, 2014, for details]. Here we have used the latter approach, and we have computed a transfer function from SSS $\psi_S(\vec{x})$ and one from SST $\psi_T(\vec{x})$ as

$$\hat{\psi}_S(\vec{k}) = \frac{|\hat{\eta}(\vec{k})|}{|\hat{S}(\vec{k})|}\hat{S}(\vec{k}) \quad \text{and} \quad \hat{\psi}_T(\vec{k}) = \frac{|\hat{\eta}(\vec{k})|}{|\hat{T}(\vec{k})|}\hat{T}(\vec{k}). \qquad (6)$$

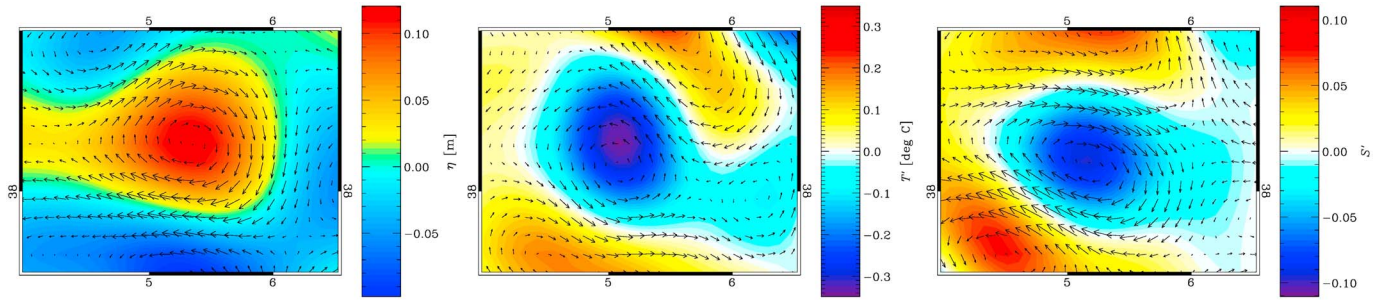

Figure 4. (left) SSH anomaly with the geostrophic velocities overplotted, (middle) SST anomaly with the velocities derived from SST, and (right) SSS anomaly with the velocities derived from SSS corresponding to 12 May 2011.

Once the surface stream function is available, surface velocities can be derived as $\vec{v}(\vec{x}) = (-\partial_y \psi, \partial_x \psi)$. Notice that, SSH is a direct estimation of the surface stream function, i.e., $\psi(\vec{x}) = g f_0^{-1} \eta(\vec{x})$. Figure 4 shows a comparison of the velocities derived from SSH, SSS, and SST during the period of the year for which there is a tendency to compensation. L4 SSS maps correctly describe the sign of buoyancy, and therefore, vorticity of Algerian eddies, while SST alone provides wrong signs because it is anticorrelated to buoyancy. An assessment of the impact of salinities on the reconstruction of velocities from SSS has been obtained through the construction of a census of vortex cores using the definition given by equation (2). To this end, we have estimated the number of anticyclonic fresh-core vortices correctly identified in L4 SSS maps, i.e., vortices with negative S' and negative circulations as derived from η and ψ_S, which have positive circulations when they are computed from ψ_T. The results shows that at least 32% of anticyclonic fresh-core eddies identified in L4 SSS maps change its polarity if they are observed with SST alone.

4. Discussion

The comparison against in situ measurements shows that the dynamical range of salinity is underestimated implying that the sensitivity is lower. This smaller dynamical range is probably an effect of the technique used for combining SST and SSS, which is a linear regression based on weighted averages on the surrounding of the point of interest [*Olmedo et al.*, 2016]. Indeed, this local averaging leads to a deterioration of small-scale gradients, although large-scale gradients are preserved. Interestingly, the typical difference of salinity between the inner part of an Algerian eddy and the outer part found from in situ measurements was ~ 0.4 [e.g., *Ruiz et al.*, 2002; *Taupier-Letage et al.*, 2003]. Therefore, the current L4 SSS are close to the limit of detection of Algerian eddies that could explain why the eddy that propagates westward disappears sooner in L4 SSS maps than in SSH and SST (see the supporting information). Nevertheless, it is worth mentioning that it is the first time that coastal eddies with signatures in salinity smaller than 0.5 have been consistently identified and tracked [see *Reul et al.*, 2014; *Umbert et al.*, 2015].

In this study we have exploited the synergy between SST and SSS to improve the space-time sampling of SSS and to enhance its quality. This approach is supported by the analysis of numerical simulations of the Mediterranean Sea that confirmed the strong tendency of the SST and SSS gradients to be aligned [*Isern-Fontanet et al.*, 2014]. Interestingly, this alignment between SST and SSS gradients has a seasonal variation [e.g., *Puillat et al.*, 2002], which is being captured by the L4 SSS maps. This is evident comparing SSS and SST anomalies within the Algerian eddies shown in Figures 2 and 4 where negative salinity anomalies correspond to positive or negative temperature anomalies depending on the period of the year. Nevertheless, the capability to capture the signature of fresh-core eddies is limited between May and September, and it is necessary to compare SSS with SSH and/or SST to separate the signature of Algerian eddies from spurious patterns. Although we do not have yet a detailed explanation of these limitations, a preliminary exploration of SMOS data suggests that the origin may come from a stronger land-sea contamination occurring during summer due to very high temperatures on land. Besides, anticyclonic eddies have a probability of $\sim$0.5 to have cold cores during summer, which may be indicative of large phase shifts between SST and SSH in summer [*Isern-Fontanet et al.*, 2014].

Our results demonstrate that SSS is of key importance to retrieve the correct polarity of Algerian eddies during summer. This points to the need to combine SSS and SST to estimate buoyancy and, then, surface velocities as already suggested by *Reul et al.* [2014]. We have attempted to compute buoyancy from SST and SSS and, then, estimate the surface stream function and currents, but the resulting velocities have been significantly different from the velocities derived from SSH. The correction of the SSS dynamical range using the parameters estimated from the comparison with in situ observations solved this limitation and provided a velocity field similar to the one provided by SSS. These results reinforces the observation that SSS is the dominant contribution to the buoyancy of Algerian eddies and, therefore, that SSS alone provides the key dynamical information that is not accessible from SST alone. Notice that the determination of buoyancy does not improve the retrieval of surface currents to respect SSS using the SQG framework if SSS and SST are in phase due to the need to fix the kinetic energy using independent observations [*Isern-Fontanet et al.*, 2008]. Finally, it is worth mentioning that the fraction of eddies that have the wrong sign of circulation if SST alone is used has been underestimated due to the limited capability to detect them in summer.

Long-term observations have unveiled a substantial increase in the loss of freshwater from the Mediterranean Sea during the last decades, which would be consistent with an increase of salinity [*Mariotti*, 2010] and appears

to drive an increase in the net water flux from the Atlantic Ocean [*Fenoglio-Marc et al.*, 2013]. Algerian eddies play a prominent role in diverting this flux of waters toward the center of the basin and, consequently, reducing the averaged salinity in the Western Mediterranean [*Isern-Fontanet et al.*, 2004]. The characterization of the nonlocal transport of fresher waters associated to these eddies requires the combined analysis of SSS and SSH. Our results show that at least during winter, SMOS measurements capture their SSS signature allowing to perform such a study. Moreover, the methods here used can, in principle, be applied to SMOS L2 data, which would provide estimations of two-dimensional surface currents with better positioning of Algerian eddies than current SSH maps allowing to overcome the sampling limitations of altimeters [*Isern-Fontanet et al.*, 2014].

5. Conclusions

In this paper it has been shown that the behavior of remotely sensed SSS anomalies is consistent with those of SST and SSH and is particularly good in winter. Moreover, the comparison between these maps and in situ salinities revealed that the SSS dynamical range is underestimated, which affects the quantitative estimates of density anomalies using SST and SSS. Despite the present technological and methodological limitations the new SSS maps can be used to obtain relevant information about the dynamics of mesoscale eddies in the Mediterranean. In particular, it has been shown that the use of SSS improves the determination of surface velocities using SQG-like approaches in comparison to SST, especially regarding the sign of vorticity.

Acknowledgments

This work has been funded by the Spanish Ministry of Economy through the National R+D Plan by means of Promises project (ESP2015-67549-C3) and previous grants and by the European Space Agency through the GlobCurrent Data User Element project (4000109513/13/I-LG). Financial support by Fundación General CSIC (Programa ComFuturo) is also acknowledged. Argo data were collected and made freely available by the Coriolis project and programs that contribute to it (http://www.coriolis.eu.org). The altimeter products were produced by Ssalto/Duacs and distributed by Aviso, with support from Cnes (http://www.aviso.altimetry.fr/duacs/). Reynolds SST were downloaded from NOAA (ftp://eclipse.ncdc.noaa.gov/pub/OI-daily-v2) and SMOS L1 data from ESA (https://earth.esa.int/web/guest/data-access/browse-data-products?selectedTags=smos.)

References

AVISO Altimetry (2012), *User Handbook Ssalto/Duacs: M(SLA) and M(ADT) Near-Real Time and Delayed-Time*, Collecte Localisation Satellites, SALP-MU-P-EA-21065-CLS ed. [Available at http://www.aviso.altimetry.fr/duacs.]

Fenoglio-Marc, L., A. Mariotti, G. Sannino, B. Meyssignac, A. Carillo, M. Struglia, and M. Rixen (2013), Decadal variability of net water flux at the Mediterranean Sea Gibraltar Strait, *Global Planet. Change*, *100*, 1–10, doi:10.1016/j.gloplacha.2012.08.007.

Font, J., et al. (2013), SMOS first data analysis for sea surface salinity determination, *Int. J. Remote Sens.*, *34*(9–10), 3654–3670, doi:10.1080/01431161.2012.716541.

Giorgi, F. (2006), Climate change hot-spots, *Geophys. Res. Lett.*, *33*, L08707, doi:10.1029/2006GL025734.

González-Haro, C., and J. Isern-Fontanet (2014), Reconstruction of global surface currents from passive microwave radiometers, *J. Geophys. Res. Oceans*, *119*, 3378–3391, doi:10.1002/2013JC009728.

Isern-Fontanet, J., E. García-Ladona, and J. Font (2003), Identification of marine eddies from altimetry, *J. Atmos. Oceanic Technol.*, *20*, 772–778.

Isern-Fontanet, J., J. Font, E. Garcia-Ladona, M. Emelianov, C. Millot, and I. Taupier-Letage (2004), Spatial structure of anticyclonic eddies in the Algerian basin (Mediterranean Sea) analyzed using the Okubo-Weiss parameter, *Deep-Sea Res. II*, *51*, 3009–3028.

Isern-Fontanet, J., B. Chapron, P. Klein, and G. Lapeyre (2006a), Potential use of microwave SST for the estimation of surface ocean currents, *Geophys. Res. Lett.*, *33*, L24608, doi:10.1029/2006GL027801.

Isern-Fontanet, J., E. García-Ladona, and J. Font (2006b), The vortices of the Mediterranean sea: an altimetric perspective, *J. Phys. Oceanogr.*, *36*(1), 87–103.

Isern-Fontanet, J., G. Lapeyre, P. Klein, B. Chapron, and M. Hetcht (2008), Three-dimensional reconstruction of oceanic mesoscale currents from surface information, *J. Geophys. Res.*, *113*, C09005, doi:10.1029/2007JC004692.

Isern-Fontanet, J., M. Shinde, and C. González-Haro (2014), On the transfer function between surface fields and the geostrophic stream function in the Mediterranean Sea, *J. Phys. Ocean*, *44*, 1406–1423, doi:10.1175/JPO-D-13-0186.1.

LaCasce, J., and A. Mahadevan (2006), Estimating subsurface horizontal and vertical velocities from sea surface temperature, *J. Mar. Res.*, *64*, 695–721.

Lapeyre, G., and P. Klein (2006), Dynamics of the upper oceanic layers in terms of surface quasigeostrophy theory, *J. Phys. Oceanogr.*, *36*, 165–176.

Mariotti, A. (2010), Recent changes in the Mediterranean water cycle: A pathway toward long-term regional hydroclimatic change?, *J. Clim.*, *23*(6), 1513–1525, doi:10.1175/2009JCLI3251.1.

Mecklenburg, S., et al. (2015), ESA's soil moisture and ocean salinity mission: From science to operational applications, *Remote Sens. Environ.*, *180*, 3–18.

Millot, C., and I. Taupier-Letage (2005), Circulation in the Mediterranean Sea, *Handbook of Environ. Chem.*, *5*(Part K), 29–66, doi:10.1007/b107143.

Olmedo, E., J. Martínez, M. Umbert, N. Hoareau, M. Portabella, J. Ballabrera-Poy, and A. Turiel (2016), Improving time and space resolution of SMOS salinity maps using multifractal fusion, *Remote Sens. Environ.*, *180*, 246–263, doi:10.1016/j.rse.2016.02.038.

Pascual, A., Y. Faugeère, G. Larnicol, and P. Le Traon (2006), Improved description of the ocean mesoscale variability by combining four satellite altimeters, *Geophys. Res. Lett.*, *33*, L02611, doi:10.1029/2005GL024633.

Puillat, I., I. Taupier-Letage, and C. Millot (2002), Algerian eddies lifetime can near 3 years, *J. Mar. Syst.*, *31*, 245–259.

Reul, N., B. Chapron, T. Lee, C. Donlon, J. Boutin, and G. Alory (2014), Sea surface salinity structure of the meandering gulf stream revealed by SMOS sensor, *Geophys. Res. Lett.*, *41*, 3141–3148, doi:10.1002/2014GL059215.

Reynolds, R., C. Smith, T. M. Liu, D. Chelton, K. Casey, and M. Schlax (2007), Daily high-resolution blended analyses for sea surface temperature, *J. Clim.*, *20*, 5473–5496.

Rio, M., A. Pascual, P. Poulain, M. Menna, B. Barceló, and J. Tintoré (2014), Computation of a new mean dynamic topography for the Mediterranean Sea from model outputs, altimeter measurements and oceanographic in-situ data, *Ocean Sci.*, *10*, 731–744, doi:10.5194/os-10-731-2014.

Ruiz, S., J. Font, M. Emelianov, J. Isern-Fontanet, C. Millot, J. Salas, and I. Taupier-Letage (2002), Deep structure of an open sea eddy in the Algerian Basin, *J. Mar. Syst.*, *33-34*, 179–195.

Taupier-Letage, I., I. Puillat, C. Millot, and P. Raimbault (2003), Biological response to mesoscale eddies in the Algerian Basin, *J. Geophys. Res.*, *108*(C8), 3245, doi:10.1029/1999JC000117.

Umbert, M., N. Hoareau, A. Turiel, and J. Ballabrera-Poy (2014), New blending algorithm to synergize ocean variables: The case of SMOS sea surface salinity maps, *Remote Sens. Environ.*, *146*, 172–187, doi:10.1016/j.rse.2013.09.018.

Umbert, M., S. Guimbard, G. Lagerloef, L. Thompson, M. Portabella, J. Ballabrera-Poy, and A. Turiel (2015), Detecting the surface salinity signature of gulf stream cold-core rings in aquarius synergistic products, *J. Geophys. Res. Oceans*, *120*, 859–874, doi:10.1002/2014JC010466.

Zweng, M. M., et al. (2013), *World Ocean Atlas 2013, Volume 2: Salinity,*edited by S. Levitus and A. Mishonov Technical, 39 pp., NOAA Atlas NESDIS 74.